

Original Article

Rabbit model of subchondral bone bruise and the treatment potential of calcitonin

Jinsong Hong^{1*}, Ting Wang^{2*}, Zhibin Chen³, Haobo Pan², Xiaohua Pan³

¹Department of Orthopedic and Traumatology, Guangzhou Orthopedic Hospital, Guangzhou China; ²Center for Human Tissue and Organ Degeneration and Shenzhen Key Laboratory of Marine Biomedical Materials, Shenzhen Institutes of Advanced Technology, China Academy of Science, Shenzhen, China; ³Department of Orthopedics and Traumatology, Bao'an Hospital Affiliated to Southern Medical University and Shenzhen Eighth People's Hospital, Shenzhen 518100, China. *Equal contributors.

Received March 30, 2017; Accepted September 3, 2017; Epub December 15, 2017; Published December 30, 2017

Abstract: Background: This study characterized a novel rabbit model of subchondral bone bruise and investigated the intervening effect of calcitonin. Methods: Bone bruise was implemented via controlled free-fall counterpoise on the medial tibial subchondral bone of 5-month-old New Zealand rabbits, with 3, 2.5, or 2 Joules of energy. Subsequent subchondral bone bruise was characterized via magnetic resonance imaging, micro computed tomography, and histology. Calcitonin was administered for 3 weeks, and the changes in subchondral bone were characterized. Results: The severity of subchondral bone bruise lesions correlated with the energy applied. The lesions involved trabecular separation and reduced trabecular number, with bone marrow edema and trabecular micro-fracture. With calcitonin treatment, subchondral bone marrow edema subsided and trabecular ultrastructure repaired. Conclusion: Free fall counterpoise is a promising method to establish a subchondral bone bruise model in rabbits. Calcitonin injection is a potential treatment for subchondral bone bruise lesions.

Keywords: Rabbits model, subchondral bone bruise, magnetic resonance imaging, calcitonin

Introduction

Subchondral bone is the layer of bone just below the cartilage in a joint, such as in the ankle, knee, hip, wrist, and shoulder. Trauma to the area, direct or indirect, can result in separation of the bone and cartilage, with bruise or bleeding from the bone into the cartilage. Subchondral bone bruise can be observed as abnormal signals on magnetic resonance imaging (MRI) [1], but is usually not observed on plain radiograph or computed tomography (CT) and is therefore frequently misdiagnosed as occult [2]. The large and complicated joints of the ankle and knee are the most frequent sites of subchondral bone bruise [3-5]. The underlying mechanism of subchondral bone bruise is still not well known. Chin et al. [6] claimed that it is induced by instability of the joint, while Sanders et al. [7] thought it the result of soft tissue injury.

The clinical study of subchondral bone bruise mainly utilizes the findings on MRI, in which on

T1WI it appears as a low intensity signal, and on T2WI as a high intensity signal [2, 8, 9]. Bone bruise lesions on fat-suppressed T2WI are shown with high sensitivity and specificity [10-12].

For basic research, there currently is no animal model of bone bruise which can closely mimic the clinical situation. Escalas et al. [13] and Ryu et al. [14] attempted to establish a bone bruise model in rabbits and pigs, respectively, by knocking the subchondral bone of knee joints. However, the applied energy could not be quantified and was not consistent. Lahm et al. [15], working with canines, used a tower to drop a weight with controlled force to observe the damage on the patella and cartilage; changes of the subchondral bone were not reported. To date, a correlation between the energy of trauma and the MRI manifestation of subchondral bone bruise has not been investigated.

Furthermore, an effective option for the treatment of subchondral bone bruise has not been

Subchondral bone bruise and calcitonin

established, nor the underlying mechanism of any treatment. Calcitonin is a hormone produced by the follicular cells of the thyroid gland, and has recently attracted interest for possible application in the treatment of subchondral bone bruise. Calcitonin functions to maintain calcium homeostasis [16], and promotes bone formation by inhibiting bone resorption by osteoclasts and bone remodeling [17]. Our clinical experience indicates that calcitonin has a positive effect in patients suffering from osteoporosis, not only for preserving bone volume, but also for recovery from subchondral bone bruise.

In the present study, we established a rabbit model of bone bruise with controlled energy, and investigated a correlation between the energy of impact and the subchondral bone bruise lesion quantified on MRI. In addition, calcitonin was administered to the established model to observe its effect on this lesion.

Material and methods

The Ethics Committee of Shenzhen People's Hospital approved all the protocols and procedures in this study.

Study design

In the first stage of this study, to establish a model of bone bruise of the knee joint, 27 New Zealand rabbits were apportioned to 3 equal groups and subjected to impacts of high, middle, or low energy (3, 2.5, and 2 Joules, respectively). The subchondral bone of the knee joints was characterized at 4 hours, 1 week, and 3 weeks by MRI, micro-CT, and histology.

Consequently, the model of bone bruise of the knee joint was established as the high-energy group ($n = 8$). An optimized dosage regimen of calcitonin (5 U/kg/day) [18] was administered daily to these rabbits for 3 weeks. The knee joints were observed and analyzed by MRI and micro-CT.

Establishment of bone bruise model

Twenty-seven New Zealand rabbits (aged 5 months, weight 2.0-2.5 kg) were randomly and equally assigned into the high-, middle-, or low-energy groups. The rabbits were anaesthetized with 10 mg/kg pentobarbital, which was slowly

injected into the auricular vein. The lower limb was fixed on a self-designed plaster brace.

The bone bruise model was established with a controlled drop weight. A hollow drop tube was fixed vertically with the outlet targeted to the edge of the cartilage at the medial side of the tibial plateau. A 0.5 kg-weight 2-cm diameter hanging-Hammer (Jinzhong Medical Machine, Shanghai China) was released for a vertical free fall through the tube at heights of 60, 50, or 40 cm to implement high-, middle-, or low-energy impacts (3, 2.5, and 2 Joules, respectively) to the medial metaphysis of the proximal tibial plateau. After the procedure, rabbits were kept in cages and free of movement.

MRI scan and analysis

The rabbits were taken for *in vivo* MRI scans at 4 hours, 1 week, and 3 weeks after injury. The rabbits were anaesthetized with 10 mg/kg pentobarbital and then fixed in an MR machine. The MRI examination was performed with a 1.5 Tesla NMR imaging scanner (Siemens). Sagittal, trans-axial fat-suppressed, and coronal fat-suppressed T2WI views were taken, each at a slice thickness of 3 mm. The sagittal scan was performed with TR 6430 ms and TE 88 ms, the trans-axial fat-suppressed scan with TR 4940 ms and TE 69 ms, and the coronal fat-suppressed scan with TR 4940 ms and TE 80 ms.

The MRI results were analyzed independently by 2 experienced radiologists. The subchondral bone was the region of interest in all 3 planes. The signal intensity was measured and the signal-to-noise ratio (SNR) was calculated as signal intensity/background noise.

Three-dimensional micro-CT analysis

At each timepoint after injury (4 hours, 1 week, and 3 weeks), 3 rabbits in each group (high-, middle-, and low-energy impact) were euthanized for micro-CT and pathohistological evaluations. The metaphysis in the proximal tibial plateau was scanned with micro-CT (SkyScan 1076, Belgium) to investigate the subchondral bone ultrastructure. During scanning, the x-ray beam was directed at the proximal tibia. The following settings were used: voxel size 18 μm , voltage 100 kV, current 100 μA , exposure time 2356 ms, frame averaging 2, and beam filtration filter 1.0 mm aluminum. Data were reco-



Figure 1. T2WI MRIs of rabbit knee joints at 4 hours, 1 week, and 3 weeks after injury. Signals of high intensity were observed at the tibial subchondral bone in the high-energy impact group at 4 hours and 1 week after the procedure (white arrow).

rded every 0.6-degree rotation step through 360 degrees. The total time per scan was 15 minutes.

After scanning, the knee joint was 3-dimensionally reconstructed with a modified Feldkamp algorithm via SkyScan reconstruction (SkyScan, Kontich, Belgium) software. The data sets for each sample were analyzed using SkyScan CT analyzer (SkyScan, Kontich, Belgium) software, with pixel size 18 μm and grey threshold 102-255. For analysis, the subchondral bone was selected as the ROI. The percent bone volume-to-total volume, trabecular thickness, trabecular separation, trabecular number, and structure model index were calculated for subchondral bone.

Pathohistological analysis

The metaphysis of the joints was harvested at 90° of flexion, fixed in 10% neutral buffered

formalin solution for 3 days, and decalcified at room temperature for 7 days with 10% formic acid. The samples were dehydrated and embedded in paraffin by the standard method. Ten serial sections were prepared from the central region of the medial tibial plateau in the sagittal plane with a thickness of 5 μm for each rabbit. Sections were alternatively used for staining with Toluidine blue. Images were captured using a Nikon H600L Microscope (Japan). Subchondral bone was observed for trabecular morphology, bone marrow bleeding or edema, and trabecular micro-fracture.

Statistical analysis

SPSS software version 13.0 (SPSS, Chicago, IL, USA) was used for all statistical analyses. Homogeneity of variance was determined by Levene's test, with $\alpha = 0.10$. The Student-Newman-Keuls' test was applied. Tamhane's T2 test was applied in the case of heterogeneity of variances. A non-parametric statistical analysis Wilcoxon test was per-

formed for comparison before and after calcitonin treatment. A P value < 0.05 was considered significant.

Results

MRI

After imposition of the injury, a high intensity signal on fat-suppressed T2-weighted images was detected in all tibial subchondral bone at each timepoint (**Figure 1**). Soft tissue injury and intra-articular effusion was obvious 4 hours after the injury at the medial side of the knee, but substantially subsided by 1 week and almost not observed at 3 weeks.

The SNR declined with time in all 3 groups (**Figure 2**). Longitudinally, the SNR intensity was positively proportional to the energy of impact, and the highest SNR was recorded for

Subchondral bone bruise and calcitonin

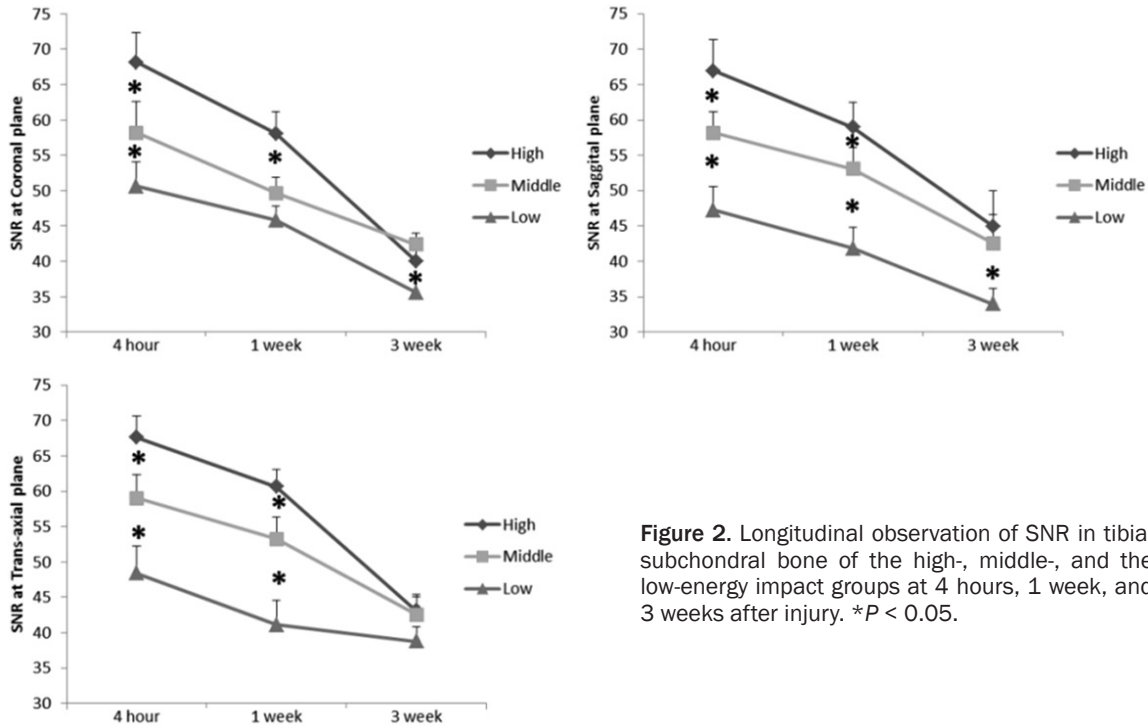


Figure 2. Longitudinal observation of SNR in tibial subchondral bone of the high-, middle-, and the low-energy impact groups at 4 hours, 1 week, and 3 weeks after injury. * $P < 0.05$.

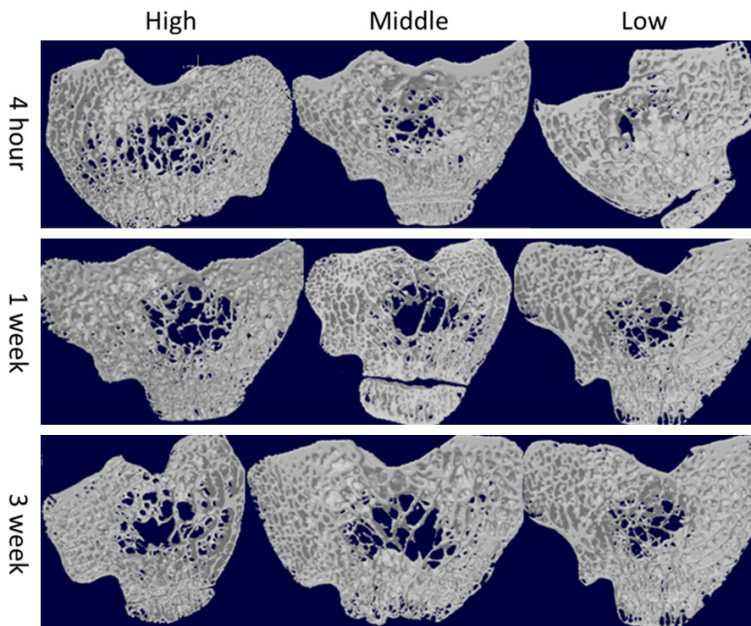


Figure 3. Three-D micro-CT images of tibial subchondral bone after injury.

the high-energy impact group. At 4 hours after injury, the SNR of the high-energy impact group in the coronal (68.16 ± 5.33), sagittal (67.62 ± 5.25), and trans-axial planes (66.91 ± 4.66) was significantly higher than that of the middle-energy (63.18 ± 5.56 , 58.99 ± 4.58 , and 58.15 ± 4.18 , respectively) and low-energy groups.

At one week after injury, the SNR of the high-energy impact group in the coronal (58.05 ± 5.25), sagittal (56.62 ± 4.65), and trans-axial planes (58.96 ± 4.78) remained significantly higher than that of the middle-energy (49.62 ± 4.44 , 53.22 ± 4.3 , and 53.06 ± 4.29 , respectively) and low-energy groups.

At 3 weeks, the SNR of the low-energy group in the coronal (33.94 ± 2.41), and sagittal (35.57 ± 2.32) planes was significantly lower than that of the high-energy and middle-energy (42.40 ± 2.75 and 42.55 ± 3.84 , respectively) groups.

Micro-CT

Micro-CT analysis was applied to observe ultrastructural changes in the tibial subchondral bone (**Figure 3**). The results showed that bone bruise did not result in significant change in bone volume or trabecular morphology.

However, the injury did induce higher trabecular separation and a reduction in trabecular num-

Subchondral bone bruise and calcitonin

Table 1. Micro-CT analysis of trabecular structure of subchondral bone of rabbit bone bruise model of high, middle and the low-energy impact groups

		High	Middle	Low	P^a	P^b	P^c
BV/TV, %	4 h	18.99 ± 2.17	18.76 ± 2.32	20.63 ± 2.09	0.832	0.778	0.256
	1 wk	21.15 ± 1.76	20.70 ± 1.72	20.77 ± 1.58	0.717	0.652	0.880
	3 wk	20.57 ± 1.85	20.52 ± 1.52	20.42 ± 1.69	0.812	0.667	0.653
Tb.Th, mm	4 h	12.49 ± 0.82	12.79 ± 1.44	12.97 ± 1.63	0.803	0.715	0.726
	1 wk	11.90 ± 1.10	12.70 ± 1.21	12.54 ± 0.95	0.664	0.536	0.587
	3 wk	13.23 ± 0.53	13.18 ± 0.93	12.32 ± 1.15	0.909	0.510	0.776
Tb.N, 1/mm	4 h	0.014 ± 0.001	0.015 ± 0.001	0.015 ± 0.002	0.231	0.213	0.199
	1 wk	0.017 ± 0.001	0.017 ± 0.001	0.019 ± 0.001	0.137	0.044	0.047
	3 wk	0.016 ± 0.001	0.016 ± 0.001	0.018 ± 0.001	0.304	0.047	0.049
Tb.Sp, mm	4 h	64.00 ± 1.08	60.96 ± 1.39	56.83 ± 1.22	0.042	0.047	0.038
	1 wk	60.11 ± 1.66	59.30 ± 1.59	56.25 ± 1.06	0.132	0.044	0.048
	3 wk	59.10 ± 1.69	60.42 ± 1.34	56.63 ± 1.36	0.205	0.044	0.047
SMI	4 h	0.39 ± 0.26	0.20 ± 0.63	0.29 ± 0.19	0.068	0.158	0.082
	1 wk	0.36 ± 0.10	0.39 ± 0.09	0.37 ± 0.10	0.017	0.228	0.178
	3 wk	0.39 ± 0.34	0.34 ± 0.28	0.26 ± 0.25	0.362	0.057	0.063

^aComparison between high- and middle-energy impact groups; ^bcomparison between high- and the low-energy impact groups; ^ccomparison between middle- and the low-energy impact groups. Abbreviations: BV/TV, percent bone volume-to-total volume; SMI, structure model index; Tb.N, trabecular number, Tb.Th, trabecular thickness; Tb.Sp, trabecular separation.

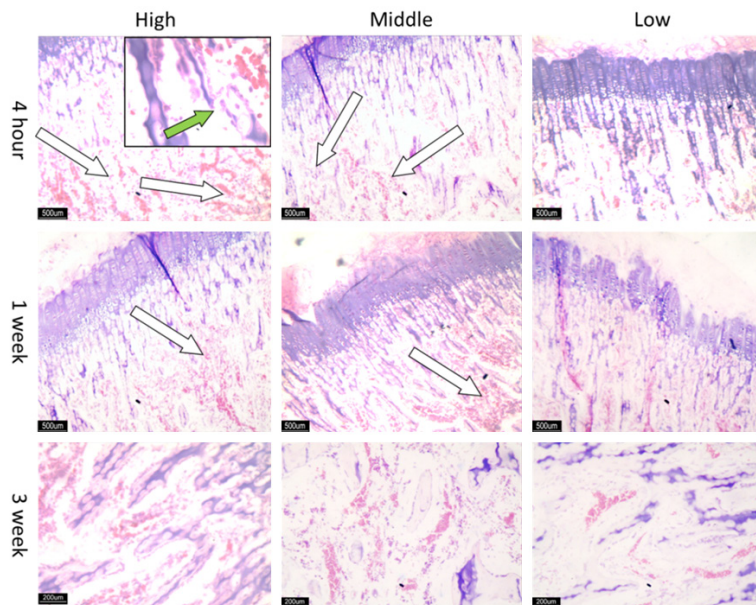


Figure 4. Pathohistological study of tibial subchondral bone after injury. Obvious subchondral bone marrow bleeding and edema were observed in the high- and middle-energy impact groups at 4 hours and 1 week (white arrows), which had dissipated by 3 weeks. In addition, trabecular micro-fracture was observed at 4 hours in the high-energy group (green arrow).

ber (Table 1). At 1 week and 3 weeks, the trabecular number of the low-energy impact group was significantly higher than that of the high- and middle-energy groups. In addition, the tra-

becular separation of the low-energy impact group was significantly lower than that of the high- and middle-energy groups at 4 hours, 1 week, and 3 weeks.

Pathohistological study

An evaluation of the morphology of the tibial subchondral bone at the cellular level was performed by pathological examination (Figure 4). Macroscopically, the articular surface and cartilage of the tibial end was intact and smooth, and the cortical bone was continuous without damage. Microscopically, bleeding of the subchondral bone marrow and edema was obvious in both the high- and middle-energy impact groups at 4 hours and 1 week, but was not observed at 3 weeks. This finding is in accord with the results of the MRI. In addition, at 4 hours after injury, trabecular micro-fracture was observed in the high-energy impact group.

Subchondral bone bruise and calcitonin

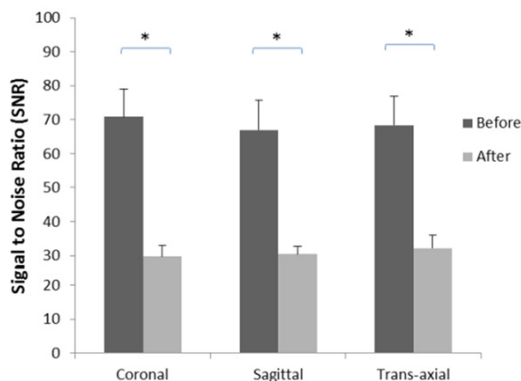


Figure 5. Comparison of SNR of knee joint subchondral bone before and after treatment by calcitonin. A strong high intensity signal observed in the MRI was greatly diminished after treatment by calcitonin for 3 weeks. After treatment, the SNR was significantly lower in the coronal, sagittal, and trans-axial planes. * $P < 0.05$.

Calcitonin treatment

After the high-energy impact group was established as the bone bruise model, we treated the rabbits with calcitonin to evaluate its effect on subchondral bone (**Figure 5**). The MRI analysis revealed that after 3 weeks of calcitonin treatment, the strong high intensity signal in the subchondral bone was greatly diminished compared with the original injury. In addition, the SNR was significantly reduced in all the coronal, sagittal, and trans-axial planes. The micro-CT analysis showed that after administration of calcitonin, the number of trabeculae decreased with greater separation, which is similar to the changes after the injury. However, it was found that the trabeculae became much thicker (**Table 2**).

Discussion

Clinically, subchondral bone bruise around a joint is common and results in pain and impaired mobility and life quality of patients. However, the underlying mechanism, pathophysiology, and treatment of subchondral bone bruise are currently not well understood. While basic research is required, a promising rabbit model of subchondral bone bruise is still lacking.

An ideal model of subchondral bone bruise should be similar to the clinical situation, that is, a closed injury to the subchondral bone around the joint, with similar pathogenesis and

pathological changes. Furthermore, the energy of the trauma should be quantified and replicable. A rabbit model should be easily and widely accessible. In the present study, the New Zealand rabbits were 5 months old, which is rather young, as they had just reached maturity [19]. We chose rabbits of this age to help diminish bone resorption by osteoclasts as a confounding factor (which increases progressively with age), allowing us to focus on the trabecular morphology and metabolism of the subchondral bone bruise lesion while the bone was at a state of homeostasis.

Based on the above criteria for an ideal model, and extensive review of previous work, we adopted the free-fall counterpoise method, by which the trauma energy is controllable and could be quantified [20]. In this study, trauma energies of 3, 2.5, and 2 Joules were chosen for the high-, middle-, and low-energy impact groups, respectively. The signal intensities on MRI were taken to reflect the severity of subchondral bone bruise lesions. By this standard, the MRI results indicated significant differences among the 3 groups at 4 hours and 1 week after the injury, with the severity of bone bruise lesions positively associated with the energy of trauma. The SNR on MRI scans of the 3 groups universally decreased with time, suggesting the pathological recovery of the lesions.

Results of the micro-CT analysis revealed that the trabecular number of the low-energy impact group was significantly higher than that of the high- and middle-energy groups, while the trabecular separation was significantly less. This may be related to differences in subchondral bone marrow hemorrhage and edema, which accelerate bone remodeling and increase reconstruction. Hemorrhage and edema may also fill the space between trabeculae, and thus increase trabecular separation.

The pathohistological study revealed obvious subchondral bone marrow hemorrhage and edema in the high- and middle-energy impact groups. This finding is in accord with the MRI results, and again suggests that the severity of subchondral bone lesion correlated with the energy of the trauma.

Currently, the clinical treatment of subchondral bone bruise focuses on the repair of soft tissue, and restraint of movement and load bearing. There is no gold standard of treatment for

Subchondral bone bruise and calcitonin

Table 2. Three-dimensional micro-CT analysis of subchondral bone ultra-structure before and 3 weeks after calcitonin treatment

	Before	After	P
Bone volume, %	13.199 ± 1.03	12.998 ± 1.89	0.079
Trabecular thickness, mm	0.164 ± 0.012	0.198 ± 0.017	0.041
Trabecular number, 1/mm	0.803 ± 0.064	0.656 ± 0.053	0.032
Trabecular separation, mm	0.921 ± 0.087	1.205 ± 0.132	0.037

subchondral bone bruise [21-23]. The successful establishment of the bone bruise model accomplished in the present study enables us to explore the treatment of subchondral bone bruise through medication. Calcitonin has been shown to regulate bone remodeling and maintain subchondral bone homeostasis, as well as effect vasodilation and increase bone mass [17, 24]. Previously, our clinical study found that calcitonin could accelerate recovery of subchondral bone bruise in patients suffering from osteoporosis (unpublished data). Therefore in the present study we further investigated the potential of this medication. Calcitonin was administered to the high-energy impact group, and after 3 weeks of treatment the MRI scans indicated significant diminishment of the subchondral bone bruise lesion compared with the original injury. This finding may bring a new perspective to the treatment of subchondral bone bruise.

The present study has several limitations. According to the principle of replacement, refinement, and reduction for research rabbits, we used a small number of rabbits, which may weaken the statistical power of the results. In addition, a vehicle group while monitoring the effect of calcitonin treatment would benefit conclusions regarding the effect of calcitonin on subchondral bone bruise lesion.

In conclusion, our study established a replicable rabbit model of subchondral bone bruise, in which lesion severity correlated with trauma energy. Furthermore, calcitonin treatment appeared to diminish subchondral bone bruise lesion in this model, which may suggest a new strategy for treatment.

Acknowledgements

This study was jointly supported by the Science and Technology Project of Shenzhen, China (GJHZ20130418150248986, JCYJ20130402-101926968, and JCYJ20150402152005636;

to Dr. XiaoHua Pan) and the Science and Technology Project of Guangzhou, China (2013J4100087 to Dr. JinSong Hong).

Disclosure of conflict of interest

None.

Address correspondence to: Dr. Xiaohua Pan, Department of Orthopedics and Traumatology, Bao'an Hospital Affiliated to Southern Medical University and Shenzhen Eighth People's Hospital, Shenzhen 518100, China. Tel: (0086) 86-13808802694, E-mail: drpxh1999@163.com

References

- [1] Mink JH, Deutsch AL. Occult cartilage and bone injuries of the knee: detection, classification, and assessment with MR imaging. *Radiology* 1989; 170: 823-829.
- [2] Ciuffreda P, Lelario M, Milillo P, Vinci R, Copolino F, Stoppino LP, Genovese EA and Macarini L. Mechanism of traumatic knee injuries and MRI findings. *Musculoskeletal surgery* 2013; 97: 127-135.
- [3] Bretlau T, Tuxoe J, Larsen L, Jorgensen U, Thomsen HS and Lausten GS. Bone bruise in the acutely injured knee. *Knee Surg Sports Traumatol Arthrosc* 2002; 10: 96-101.
- [4] Rubin DA, Harner CD, Costello JM. Treatable chondral injuries in the knee: frequency of associated focal subchondral edema. *AJR Am J Roentgenol* 2000; 174: 1099-1106.
- [5] Vincken PW, Ter Braak BP, van Erkel AR, Coerkamp EG, Mallens WM and Bloem JL. Clinical consequences of bone bruise around the knee. *European radiology* 2006; 16: 97-107.
- [6] Chin YC, Wijaya R, Chong le R, Chang HC and Lee YH. Bone bruise patterns in knee injuries: where are they found? *Eur J Orthop Surg Traumatol* 2014; 24: 1481-1487.
- [7] Sanders TG, Medynski MA, Feller JF and Lawhorn KW. Bone contusion patterns of the knee at MR imaging: footprint of the mechanism of injury. *Radiographics* 2000; 20: 135-51.
- [8] Yao L, Lee JK. Occult intraosseous fracture: detection with MR imaging. *Radiology* 1988; 167: 749-751.
- [9] Davies NH, Niall D, King LJ, Lavelle J and Healy JC. Magnetic resonance imaging of bone bruising in the acutely injured knee—short-term outcome. *Clin Radiol* 2004; 59: 439-445.
- [10] Lal NR, Jamadar DA, Doi K, Newman JS, Adler RS, Uri DS and Kazerooni EA. Evaluation of bone contusions with fat-saturated fast spin-

Subchondral bone bruise and calcitonin

- echo proton-density magnetic resonance imaging. *Can Assoc Radiol J* 2000; 51: 182-185.
- [11] Mirowitz SA, Apicella P, Reinus WR, Hammerman AM. MR imaging of bone marrow lesions: relative conspicuousness on T1-weighted, fat-suppressed T2-weighted, and STIR images. *AJR Am J Roentgenol* 1994; 162: 215-221.
- [12] Arndt WF 3rd, Truax AL, Barnett FM, Simmons GE and Brown DC. MR diagnosis of bone contusions of the knee: comparison of coronal T2-weighted fast spin-echo with fat saturation and fast spin-echo STIR images with conventional STIR images. *AJR Am J Roentgenol* 1996; 166: 119-124.
- [13] Escalas F, Curell R. Occult posttraumatic bone injury. *Knee Surg Sports Traumatol Arthrosc* 1994; 2: 147-9.
- [14] Ryu KN, Jin W, Ko YT, Yoon Y, Oh JH, Park YK and Kim KS. Bone bruises: MR characteristics and histological correlation in the young pig. *Clin Imaging* 2000; 24: 371-380.
- [15] Lahm A, Uhl M, Edlich M, Erggelet C, Haberstroh J and Kreuz PC. An experimental canine model for subchondral lesions of the knee joint. *Knee* 2005; 12: 51-5.
- [16] Pondel M. Calcitonin and calcitonin receptors: bone and beyond. *Int J Exp Pathol* 2000; 81: 405-422.
- [17] Kauther MD, Bachmann HS, Neuerburg L, Broecker-Preuss M, Hilken G, Grabellus F, Koehler G, von Knoch M and Wedemeyer C. Calcitonin substitution in calcitonin deficiency reduces particle-induced osteolysis. *BMC Musculoskelet Disord* 2011; 12: 186.
- [18] Kuo YJ, Tsuang FY, Sun JS, Lin CH, Chen CH, Li JY, Huang YC, Chen WY, Yeh CB and Shyu JF. Calcitonin inhibits SDCP-induced osteoclast apoptosis and increases its efficacy in a rat model of osteoporosis. *PLoS One* 2012; 7: e40272.
- [19] Achari Y, Reno CR, Tsao H, Morck DW and Hart DA. Influence of timing (pre-puberty or skeletal maturity) of ovariectomy on mRNA levels in corneal tissues of female rabbits. *Mol Vis* 2008; 14: 443-455.
- [20] Newberry WN, Garcia JJ, Mackenzie CD, Decamp CE and Haut RC. Analysis of acute mechanical insult in an animal model of post-traumatic osteoarthritis. *J Biomech Eng* 1998; 120: 704-709.
- [21] Vannet N, Kempshall P, Davies J. Secondary collapse of lateral femoral condyle following bone bruise: a case report. *Acta Orthop Belg* 2009; 75: 695-698.
- [22] Green DM, Noble PC, Bocell JR Jr, Ahuero JS, Poteet BA and Birdsall HH. Effect of early full weight-bearing after joint injury on inflammation and cartilage degradation. *J Bone Joint Surg Am* 2006; 88: 2201-2209.
- [23] Wright RW, Phaneuf MA, Limbird TJ and Spindler KP. Clinical outcome of isolated subcortical trabecular fractures (bone bruise) detected on magnetic resonance imaging in knees. *Am J Sports Med* 2000; 28: 663-667.
- [24] Lassen LH, Jacobsen VB, Haderslev PA, Sperling B, Iversen HK, Olesen J and Tfelt-Hansen P. Involvement of calcitonin gene-related peptide in migraine: regional cerebral blood flow and blood flow velocity in migraine patients. *Th J Headache Pain* 2008; 9: 151-157.